



Effects of spectral light quality and carbon dioxide on the physiology of *Micractinium inermum*: growth, photosynthesis, and biochemical composition

Kathryn E. Dickinson¹ · Crystal G. Lalonde¹ · Patrick J. McGinn¹

Received: 17 April 2019 / Revised and accepted: 22 July 2019 / Published online: 17 August 2019
© Crown 2019

Abstract

Growth, photosynthetic parameters, and biochemical composition of the chlorophyte *Micractinium inermum* were determined under conditions of different light-emitting diode (LED) wavelength distributions and carbon dioxide (CO₂) levels of 1, 5, and 10% v/v. Increasing the inflowing CO₂ concentration from 1 to 5 to 10% had negative effects on maximum growth rate (μ_{\max}), relative growth rate (RGR), biomass production, and CO₂ fixation rate. Cultures subjected to a spectral distribution containing a blue wavelength peak were less negatively affected than red as CO₂ stress increased, and evidently there was a quantitative effect depending on the peak area percentage. Under non-stressful conditions (1% CO₂), there were no significant differences in μ_{\max} or RGR among light treatments; however, blue light resulted in decreased lag phases (0.75 less days than red). Biomass production was significantly higher in red wavelength peak treatments at 1% CO₂ (i.e., monochromatic red treatment = $0.772 \pm 0.07 \text{ g L}^{-1}$) which demonstrates that although blue light allows for an early growth advantage, cultures grown with red light are able to catch up and result in more biomass. At a 10% CO₂ level, RGR was higher in treatments with blue peaks; red peak treatments were no longer able to overcome the stress and demonstrated lag phases 4.87 days longer than blue peak treatments. Inhibition of photosystem II function was evident as CO₂ concentrations increased. Evaluation of biochemical composition revealed that protein content was significantly greater in blue peak treatments at 10% CO₂, pigment content was up to 2× greater than red at all CO₂ levels, and total FAME and fatty acid profiles did not exhibit major changes.

Keywords *Micractinium inermum* · Chlorophyta · Algae · Carbon dioxide · Wavelengths · Composition · Photochemistry · Growth · Spectral quality · LED

Introduction

The potential for large-scale microalgal production is gaining commercial traction due to the ability of these photosynthetic organisms to convert carbon dioxide into valuable biomass with a variety of uses such as for bioenergy, fertilizer, nutraceuticals, and bioplastics (Ruiz et al. 2016). Rapid advances in algal biotechnology, depleting non-renewable resources, and increasing CO₂ levels adding to greenhouse gas

(GHG) emissions are driving forces behind clean technologies such as industrial-scale algal production (Wijffels and Barbosa 2010). Commercial-level production is still in its initial stages with many factors affecting culture growth kinetics, targeted biomolecules, and quality of biomass that have yet to be optimized.

Carbon sequestration into biomass can “recycle” or in part offset industrial GHG emissions, and industries investigating means of decreasing their carbon footprint are recently considering microalgal production using flue gas as the carbon source for growth (Pires et al. 2012; Kumar et al. 2014a). Operationally, there are many challenges associated with mass cultivation of microalgae on flue gas emissions particularly because CO₂ levels can fluctuate daily and even halt for periods of time. Thus, mitigating backup systems need to be in place to prevent system crashes and poor growth.

Generally CO₂ is present in flue gas at a concentration between 3 and 15% (Packer 2009), a range at which a variety of fast-growing microalgae have been shown to tolerate to different

Electronic supplementary material The online version of this article (<https://doi.org/10.1007/s10811-019-01880-z>) contains supplementary material, which is available to authorized users.

✉ Kathryn E. Dickinson
Katie.Dickinson@nrc-cnrc.gc.ca

¹ Aquatic and Crop Resources Development, National Research Council of Canada, 1411 Oxford St., Halifax, NS B3H 3Z1, Canada

extents. Cuellar-Bermudez et al. (2015) present such a comparison of microalgal strains including those of *Chlorella*, *Scenedesmus*, *Botryococcus*, and *Nannochloropsis* which demonstrates varying degrees of tolerance to CO₂ levels from ambient air up to 50%. Management of CO₂ recycling would be greatly aided by an improved understanding and selection of choice strains tolerant to varying CO₂ levels. Determining optimal conditions for fast growth and high biomass yield would allow for selection of strains with the greatest carbon fixation potential.

Photosynthesis is the only way to produce energy from light and carbon dioxide (Janssen et al. 2002) and the capability to fix CO₂ should be positively correlated with their light utilization efficiency (Pires et al. 2012). Light supply (i.e., intensity, spectra, source, etc.) therefore plays an important role in photobioreactor (PBR) design, and in regions where sunlight availability is unreliable, it is essential to develop enclosed photobioreactors with an artificial light source provided. Cost and productivity, however, remain the two fundamental barriers to commercialization (Pienkos and Darzins 2009). Increasing advances in lighting technology, such as light-emitting diodes (LEDs), allows for numerous options for photobioreactors; LEDs have a lower energy demand than fluorescent lights, have a longer lifetime (~50,000 h), and emit nearly monochromatic light at various wavelengths (Baer et al. 2016). With the ability to apply and select a narrow range of emissions spectra to a PBR design, less energetic photons can be applied in an effort to decrease production cost. For example, because blue photons are more energetic than red photons, more photons are released by LEDs emitting at longer wavelengths than for LEDs emitting at shorter wavelengths (Shultze et al. 2014) and therefore with less voltage used by the LED. The application of monochromatic red light has been desirable for this reason, and many groups have chosen this method. Red light within wavelengths of 600–700 nm is generally the most efficient for photosynthesis; however, it has been suggested that blue light between 400 and 500 nm may be required for other metabolic processes besides photosynthesis (Carvalho et al. 2011). There are known interactive effects between light quantity, quality, and CO₂ concentrations on microalgal growth, although these are not completely understood. It is known that the ability of microalgae to assimilate inorganic carbon from the environment is influenced by the CO₂-concentrating mechanism (CCM) and that at higher CO₂ concentrations (1% and greater), this mechanism is repressed (Beardall et al. 1998). Borodin et al. (1994) reported that adaptation to air levels of CO₂ from high CO₂ was more efficient under blue, compared with red, light. In *Chlorella vulgaris*, it was shown that, in addition to a low CO₂ concentration, blue light was necessary to induce carbonic anhydrase, an enzyme critical to CCM function in microalgae (Umino et al. 1991). Borodin et al. (1994) also observed a difference between cells adapted to

blue light versus red light under inorganic carbon-saturating conditions, with blue light grown cells having a higher affinity for CO₂. Less is known about the interactions between light quality and higher CO₂ levels that are detected in flue gases and the interactions at play with other environmental variables. It has been demonstrated that increasing CO₂ concentrations have positively correlated with biomass yield (Tang et al. 2011; Pires et al. 2012); however, the results and tolerance levels differ greatly among microalgal strains. In an industry where maximal productivity is sought, whether productivity means increased algal biomass, a particular biochemical component, increased carbon fixation, and/or gas production etc., any variable change that can offer an improvement to culture growth should be considered.

Micractinium inermum (SMC-5F) is considered a potential candidate for industrial-scale growth based on meeting initial screening criteria of high growth rate and cell yield, on par with other green algae such as the closely related *Chlorella* and *Scenedesmus*. To date, however, little is known on the effects of CO₂ concentration on *Micractinium* sp. (Kumar et al. 2014b) and there is no information available on spectral specificity on growth or photosynthetic characteristics of *M. inermum*. In a search for strains with advantages or tolerances to specific environmental conditions which could additionally lead to unique biochemical profiles, *M. inermum* was deemed a candidate worthy of further study. The objective of the study was to investigate different CO₂ concentrations and light qualities on the biomass productivity maintained at a constant irradiance rate, as it pertains to large-scale photobioreactor application.

Materials and methods

Strain and culture conditions

Micractinium inermum (SMC-5F) was isolated from freshwater samples from Trout Creek, St. Marys, Ontario, Canada (N43° 15.709/W081° 08.181). The isolate was identified by DNA sequence analysis of 18S, ITS1, and ITS2 regions (Eurofins Genomics, Huntsville, AL, USA) and has been maintained in our on-site phytoplankton collection. Initial flask cultures were grown under the experimental light conditions and were continuously bubbled with an air and CO₂ mixture at a CO₂ concentration of 2% v/v. Experimental photobioreactors (500 mL) were inoculated from the initial flasks to a cell concentration of 1×10^5 cells mL⁻¹ and were cultivated at 20 °C in duplicate 0.5-L photobioreactors containing tangentially filtered and autoclaved lake water amended with NaNO₃ 4.41×10^{-3} M, NaH₂PO₄ H₂O 1.81×10^{-4} M, and f/2 trace metal and vitamin solutions (Guillard and Ryther 1962). Photobioreactors were mixed using a shaker table set at 100 rpm, and cultures were bubbled with air and

CO₂ blends of various concentrations of CO₂, 1, 5, and 10%, and delivered at a flow rate of 0.1 L min⁻¹.

LED light strips consisting of 60 diodes, 5 rows of 12, continuously illuminated the vessels and provided an irradiance rate of 50 μmol photons m⁻² s⁻¹ (established by taking the mean of 9 points along a horizontal transect across the vessel filled with water) using a Biospherical Instruments Inc. QSL-2100 (USA) scalar PAR irradiance sensor. We grew the cultures at a low, light-limiting intensity to approximate low light availability in commercial-scale photobioreactors. Six different light quality treatments were applied using red, blue, and green LEDs. The 3 LEDs were applied independently to provide monochromatic light, and blended to provide mixes, as shown in Table 1. The emission spectra (Fig. 1) were measured using a high-resolution Flame spectrometer (Ocean Optics Inc., USA).

Photosystem parameters

Chlorophyll fluorometry and data analysis were conducted using a Fluorescence Induction and Relaxation System FIRE fluorometer (Satlantic, Canada), the FIREWORX script (Audrey Barnett, <http://sourceforge.net/projects/fireworx/>), and the flash lamp calibration factors provided by Satlantic. Fluorescence induction curves detected at a wavelength of 678 nm were generated by applying a saturating single turnover flash (STF, 80 μs) of blue light (455 nm with 30 nm bandwidth) to estimate minimum (F_o) and maximum fluorescence (F_m). The STF causes photons to be delivered to the PSII antenna, causing the PSII reaction centers to close and therefore generate an increase in fluorescence. Fluorometry measurements for F_o and F_m were taken from cells that were dark acclimated for at least 20 min. Actinic light was applied at a rate of 50 μmol photons m⁻² s⁻¹ for 1 min to determine quantum yield of photochemistry in PSII (Φ PSII), photochemical quenching (qP), and non-photochemical quenching (NPQ). Maximum quantum yield of PSII (F_v/F_m) was calculated as $(F_m - F_o)/F_m$, Φ PSII was calculated as $(F_m' - F_o)/F_m'$, and we estimated qP as $(F_m' - F_o)/(F_m' - F_o')$ and NPQ as $(F_m - F_m')/F_m'$.

Table 1 Spectral light treatments of blue, red, and green light emitting diodes. Ratios confirmed using a high-resolution Flame spectrometer (Ocean Optics Inc., FL, USA)

Abbreviation	Treatment
B	Blue
R	Red
W	White; red 3: green 2: blue 3
M1	Red 20: blue 1
M2	Red 10: blue 1
M3	Red 2: blue 1

Analytical procedures

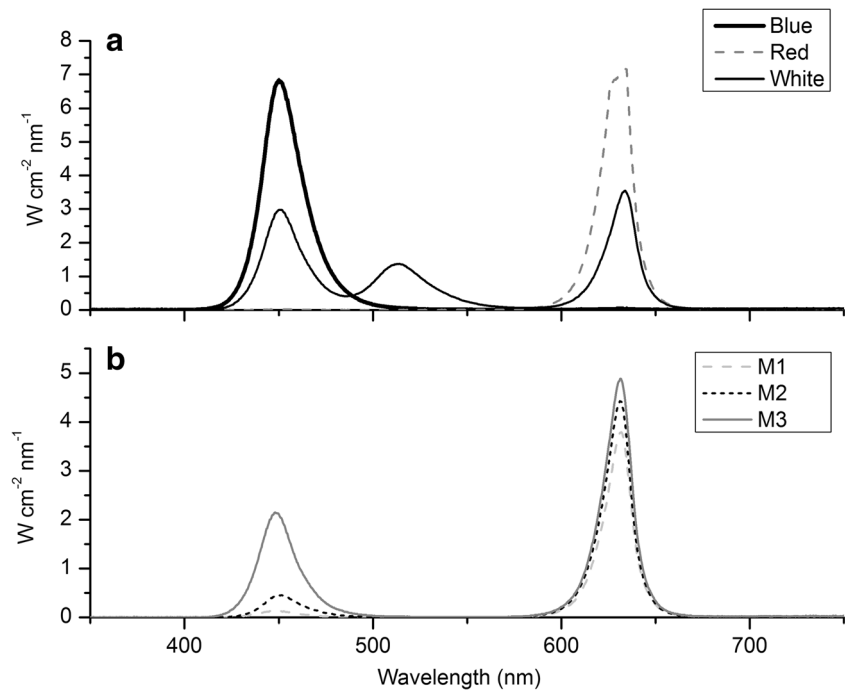
Specific maximum growth rates (μ_{max}) and relative growth rates (RGR) were determined by μ (day⁻¹) = $(\ln C_2 - \ln C_1)/(T_2 - T_1)$, where C_2 and C_1 are the cell densities sampled at times T_2 and T_1 , respectively. Maximum growth rates were calculated from the linear regression of three consecutive points where the maximum growth rate equals the slope of that line. Relative growth rates were calculated from day 0 to the stationary phase (no change in growth from the previous day), which captures the lag and exponential phases of growth.

The CO₂ fixation rate was determined from the carbon content of algal cells and the biomass productivity (BP) as follows: $R_{CO_2} = C_c \times BP \times (M_{CO_2}/M_C)$; where R_{CO_2} is the CO₂ fixation rate (g CO₂ L⁻¹ day⁻¹), BP is the biomass productivity (g dry cell weight per liter per number of days of growth), and M_{CO_2} and M_C are the molecular weights of CO₂ and elemental carbon, respectively. C_c is the carbon content (g carbon per g dry cell weight) (Yun et al. 1997).

Cell densities were monitored daily using a Multisizer 4 Coulter Counter (Beckman, USA), and dry weights were determined according to Dickinson et al. (2013). Algae were harvested at mid-exponential and early stationary phases, and were filtered according to Dickinson et al. (2013) and centrifuged to pellet form (Thermo Scientific Sorvall Legend X1R, USA), immediately frozen at -80 °C, lyophilized (Labconco FreeZone 4.5, USA), and stored at -80 °C prior to conducting elemental (carbon, nitrogen), fatty acid, and pigment analyses.

Ash levels were determined gravimetrically by combusting pre-weighed dry biomass in a muffle furnace at 550 °C and averaged ~1%. Total carbon (C) and nitrogen (N) were measured by elemental analysis using a vario Micro cube (Elementar Americas Inc., USA) standardized with sulfanilamide. The nitrogen-to-protein (N-to-P) factor used to estimate protein content was 4.78 (Lourenço et al. 2004). This approach has been found to be valid and it decreases the potential for analytical issues that can occur with protein extraction processes (Laurens et al. 2012; Tibbetts et al. 2015a). In addition, this N-to-P factor is highly similar (N × 4.86) to that previously reported for a related *Micractinium* strain (*M. reisserii*) by Tibbetts et al. (2015b). Total fatty acid methyl ester (FAME) concentrations and fatty acid (FA) profiles were determined using a methanolic HCl in situ transesterification extraction method and analyzed on a gas chromatograph that was equipped with flame ionization detection (Agilent 7890, USA) and separated on an Omegawax 250 capillary column. PUFA-3 and Supelco-37 (Sigma-Aldrich Canada Co., Canada) were used as external standards, and C19:0 (methyl nonadecanoate, Sigma-Aldrich Canada Co.) was the internal standard added to each sample prior to transesterification for calibration purposes. Carbohydrate was calculated by

Fig. 1 Spectral distributions of light treatments obtained using a high resolution Flame spectrometer (Ocean Optics USA) for **a** red, blue, and white treatments and **b** M1, M2, and M3 treatments



difference [100 – (total FA, crude protein + ash)]. Working in dim light, pigments were extracted with 90% acetone, sonicated with sea sand for 1 h in an ultrasonic bath (Ney, Ultrasonik 57x, USA), kept at -20°C overnight, and centrifuged at $684\times g$ for 5 min. Chlorophyll *a* and *b* and total carotenoids in the extracts were determined using a Genesys 10 UV-Vis spectrophotometer and using the extinction coefficients of Jeffrey and Humphrey (1975) and Strickland and Parsons (1968). Absorption spectra were determined using extracts from the blue, red, and white light treatments normalized for cell density (Fig. 2). All values reported are means of three analytical replicates from each of the two

biological replicates except for total fatty acid which is a mean of two replicates.

Statistical methods

Statistical analyses were carried out using OriginPro 8, and the statistical significance level was $p < 0.05$. Data were assessed for interactions using two-way ANOVA with light and CO_2 treatments as the sources of variance. All data were checked and were significantly drawn from a normally distributed population at the 0.05 level using the Kolmogorov-Smirnov test. One-way ANOVA followed by post hoc Tukey's tests were applied to test for differences.

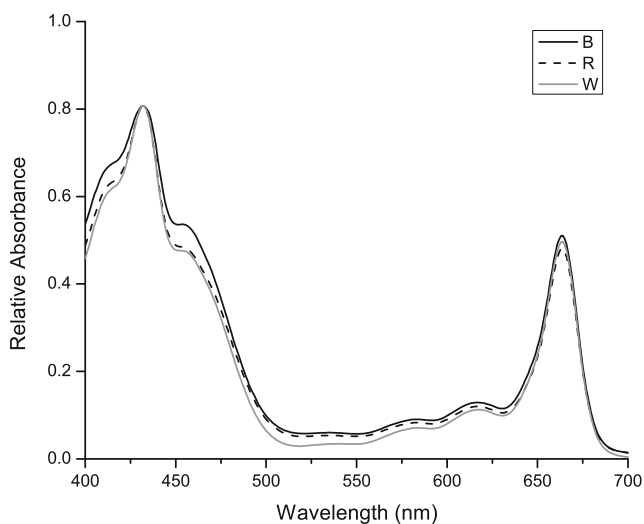


Fig. 2 Absorption spectra of *Micractinium inermum* cells taken from blue, red, and white LED treatment cultures, extracted in 90% acetone

Results

The green microalga *Micractinium inermum* was grown in air enriched with CO_2 to final concentrations of 1, 5, or 10% (v/v). Under each CO_2 treatment, cultures were grown in the presence of white (W), blue (B), or red (R) light or a combination of R and B light (M1, M2, M3; see Table 1 and Fig. 1 for spectral characteristics of different growth light treatments). The growth rate of *M. inermum* was strongly dependent on the CO_2 concentration provided for growth. Overall, the highest growth rates were observed under 1% CO_2 and generally decreased as it was increased to 5 and 10% (Table 2). The lowest growth rates were observed in cultures grown in the presence of 10% CO_2 . Interestingly, the lag period observed before onset of the exponential phase increased as CO_2 increased, with

Table 2 Maximum growth rate (μ_{\max}), the time frame of achieved μ_{\max} based on linear regression and relative growth rate (day^{-1}) for *Micractinium inermum* under different CO₂ concentrations and LED treatments. Data represent means ($n = 4 \pm \text{SD}$)

CO ₂ conc.		B	R	W	R20/B1	R10/B1	R2/B1	<i>p</i>
1%	μ_{\max} (day^{-1})	1.34 ± 0.06a	1.42 ± 0.04a	1.58 ± 0.08a	1.48 ± 0.13a	1.51 ± 0.01a	1.40 ± 0.04a	0.115
	μ_{\max} time points (days)	0–1.79	0.75–2.75	0–1.79	0.75–2.75	0.75–2.75	0–1.79	
	Rel. μ (day^{-1})	0.64 ± 0.04a	0.58 ± 0.01a	0.59 ± 0.01a	0.59 ± 0.01a	0.59 ± 0.01a	0.59 ± 0.02a	0.113
5%	μ_{\max} (day^{-1})	1.36 ± 0.01 ac	1.07 ± .02b	1.61 ± 0.20c	0.96 ± 0.13a	1.18 ± 0.11abc	1.25 ± 0.14abc	0.016
	μ_{\max} time points (days)	1.08–3.22	3.22–5.10	1.08–3.22	2.21–4.02	2.21–4.02	1.08–3.22	
	Rel. μ (day^{-1})	0.48 ± 0.01a	0.55 ± 0.02b	0.47 ± 0.02b	0.56 ± 0.05a	0.53 ± 0.01a	0.48 ± 0.01b	0.029
10%	μ_{\max} (day^{-1})	0.87 ± 0.11ab	0.64 ± 0.45 ac	1.06 ± 0.01b	0.21 ± 0.15c	0.90 ± 0.04ab	0.72 ± 0.17ab	0.011
	μ_{\max} time points (days)	5.96–7.79	10.83–13.01	5.96–7.79	10.83–13.01	10.83–13.01	5.96–7.79	
	Rel. μ (day^{-1})	0.43 ± 0.01a	0.30 ± 0.09b	0.44 ± 0.01a	0.09 ± 0.06	0.37 ± 0.04a	0.40 ± 0.00a	0.009

Values within the same row having different lowercase letters are significantly different ($p < 0.05$)

the longest lag periods observed in cultures grown in 10% CO₂ irradiated with red light alone or in treatments with a high proportion of red light (M1, M2; Table 2).

Cultures that depended on air alone grew very slowly and after 10 days had produced less than one tenth the cell density of the 1% CO₂ treatment (data not shown). Statistical interactions were found between light quality and CO₂ for relative growth rate ($p < 0.001$), productivity during the exponential phase ($p < 0.001$) and during stationary ($p < 0.001$) using two-way ANOVA statistical analysis. Maximum growth rate did not have a significant interaction between LED and CO₂ treatments ($p = 0.098$); however, the individual factors, across light treatments and CO₂ treatments, were significant ($p < 0.001$ and $p < 0.001$, respectively). The results of these comparisons are presented in Tables 2, 3, and 4. Under 1% CO₂, there are no significant differences in μ_{\max} or RGR as a function of the growth light regime. Under both 5 and 10% CO₂ where growth is increasingly inhibited, spectra including blue light demonstrate higher μ_{\max} than in red light or with a high proportion of red light (M1, M2) (Table 2.). At 5% CO₂, although blue light treatments had greater μ_{\max} , red light cultures were able to catch up and resulted in higher relative growth rates overall. With additional stress at 10% CO₂ concentrations, B, W,

and M3 treatments resulted in greater μ_{\max} and RGR than R, M1, and M2. At 5 and 10% CO₂ concentrations, W (a mixture of blue, green, and red light) demonstrated a significantly higher μ_{\max} than the other light treatments. Interestingly, in addition to the growth rate yields mentioned, light had a significant effect on growth kinetics in terms of lag time. Even with 1% CO₂, red light and high red light ratios (M1, M2) demonstrated a slightly longer lag phase than those with greater blue wavelength peaks (B, W, M3). As CO₂ concentrations increased, the lag phase increased across the board but had a much greater effect on red light treatments (R, M1, M2). In the case of 10% CO₂, the lag phase lasted 5.96 days for B, W, and M3 and 10.96 days for R, M1, M2. After such a long lag phase, some cultures did not survive as was the case with one R and both M1 replicates (Table 2).

In terms of biomass production, the greatest yields were observed under 1% CO₂ in the early stationary phase irrespective of light regime (Fig. 3). However, there were no significant differences in biomass yields between 1 and 5% CO₂ for the R, M1, and M2 treatments. W resulted in the most biomass during the exponential phase at all CO₂ levels and during the stationary phase at 1 and 10%. The μ_{\max} from the 5% CO₂ treatment was greater with high blue light peaks (B, W, M3) than the high red light peaks (R, M1, and M2), and the lag

Table 3 CO₂ fixation rate ($\text{g CO}_2 \text{ L day}^{-1}$) for *Micractinium inermum* under different CO₂ concentrations and LED treatments determined using the calculation indicated in “Materials and methods.” Data represent means ($n = 6 \pm \text{SD}$)

	B	R	W	R20/B1	R10/B1	R2/B1	<i>p</i>
1%	0.15 ± 0.02a	0.17 ± 0.02a	0.17 ± 0.02a	0.16 ± 0.04a	0.14 ± 0.03a	0.14 ± 0.03a	0.731
5%	0.09 ± 0.01a	0.12 ± 0.01b	0.08 ± 0.01a	0.11 ± 0.01ab	0.10 ± 0.03ab	0.08 ± 0.00a	0.023
10%	0.07 ± 0.01 ac	0.04 ± 0.01bc	0.07 ± 0.02 ac	ND	0.06 ± 0.00 ac	0.05 ± 0.01 ac	0.019

Values within the same row having different lowercase letters are significantly different ($p < 0.05$)

ND no data

Table 4 Protein content of *Micractinium inermum* under different CO₂ concentrations and LED treatments during exponential and stationary phases. Data represent means ($n > 4 \pm SD$)

Protein % dw		B	R	W	R20/B1	R10/B1	R2/B1	<i>p</i>
1%	Exp.	45.3 ± 0.4a	46.1 ± 0.7a	45.2 ± 1.0a	48.1 ± 1.3b	46.8 ± 1.4abc	44.9 ± 0.5 ac	0.004
	Stat.	38.9 ± 0.7a	28.6 ± 2.0b	34.1 ± 2.9 ac	33.4 ± 2.6c	34.5 ± 2.2 ac	35.3 ± 0.9 ac	< 0.001
5%	Exp.	38.6 ± 0.7 ac	39.5 ± 0.8a	37.3 ± 0.9bc	39.4 ± 0.1a	37.2 ± 0.2bc	37.9 ± 0.6c	< 0.001
	Stat.	31.1 ± 2.8ab	29.5 ± 1.8ab	34.0 ± 0.6a	27.7 ± 1.0b	31.6 ± 1.2ab	31.5 ± 2.0ab	0.020
10%	Exp.	40.9 ± 0.0a	34.1 ± 1b	37.6 ± 0.3c	37.6 ± 0.1c	38.0 ± 1.5c	41.9 ± 0.6bc	< 0.001
	Stat.	38.3 ± 0.6a	33.2 ± 2.1b	33.1 ± 2.5b	ND	41.7 ± 1.0a	40.8 ± 0.4a	< 0.001

Values within the same row having different letters are significantly different ($p < 0.05$)

ND no data

phase was much shorter (Table 2); however, the maximum cell density was significantly suppressed ($p < 0.001$).

Carbon dioxide fixation rate was calculated as described in “Materials and methods,” and there was a significant interaction observed between CO₂ and LED treatments ($p = 0.0057$). Faster CO₂ fixation occurred at 1% CO₂ with no significant differences found among LED treatments (Table 3). With increasing CO₂ concentration, there is a decrease in CO₂ fixation rate ($p < 0.001$). There are no significant differences among LED treatments overall ($p = 0.361$, two-way ANOVA) although variations are evident when examined individually with Tukey’s post hoc test, as was shown with 10% CO₂ where one R and both M1 replicates did not survive (Table 3).

Maximum quantum yield of photosystem II (PSII) was affected by both CO₂ concentration and spectral distribution ($p < 0.001$, $p < 0.001$), and there was no significant interaction between the two ($p = 0.018$). Across all light treatments, the

index of maximum photochemical efficiency of PSII (F_v/F_m) decreased as CO₂ concentrations increased ($p < 0.001$) (Fig. 4). Photochemical quenching (qP), the degree to which reaction centers are open or closed, and ϕ PSII, which reveals the photochemical yield of electron transport of open PSII reaction centers (Chaloub et al. 2010), did not change significantly between 1 and 5% CO₂ but decreased with the 10% treatment ($p = 0.006$, $p < 0.001$, respectively). Maximum quantum yields demonstrated significant evidence to a quantitative trend that a blue wavelength peak led to slightly increased levels at 1% CO₂ (Fig. 4). With the addition of environmental stress, seen at 10% CO₂, F_v/F_m became significantly suppressed in the light treatments containing higher red ratios (R, M1, M2) and a similar trend could be seen with ϕ PSII ($p = 0.008$ and $p = 0.002$, respectively) (Fig. 4). Although non-photochemical parameters were measured, a methodological problem occurred where F_m was lower than the F_m' level taken at growth light intensity. We therefore

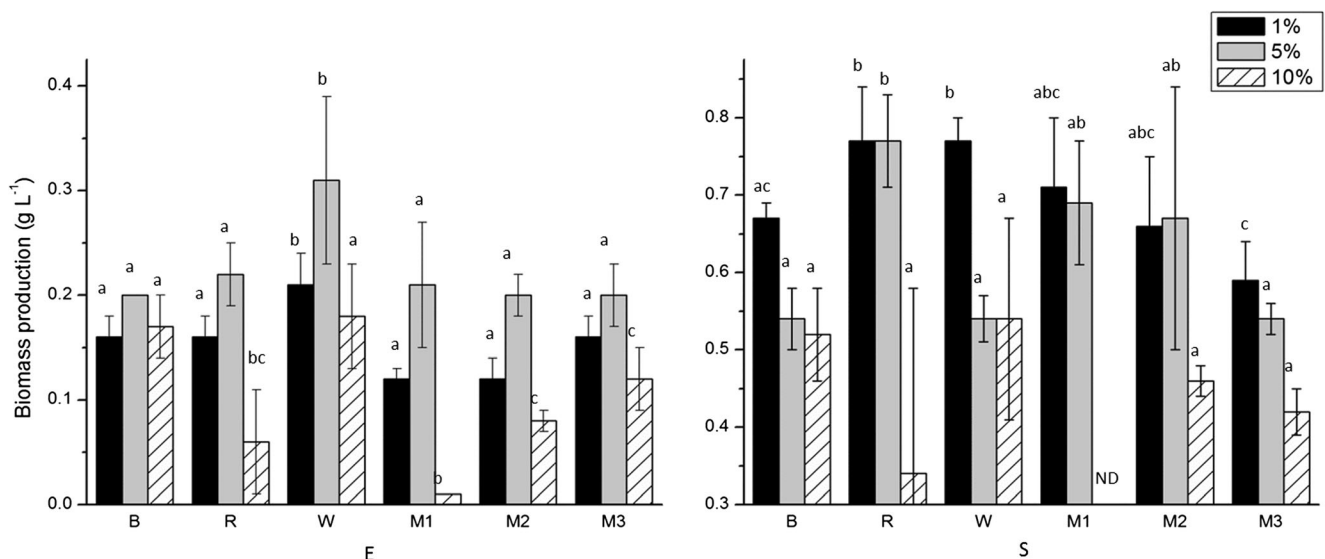


Fig. 3 Biomass production (g L^{-1}) for *Micractinium inermum* under 3 different CO₂ concentrations (1%, 5%, and 10%) and 6 LED treatments during the exponential (E, column on the left) and stationary phases (S,

column on the right). Data represent means ($n = 6 \pm SD$). Values within the same bar pattern with different letters represent a significant difference ($p < 0.05$). ND no data

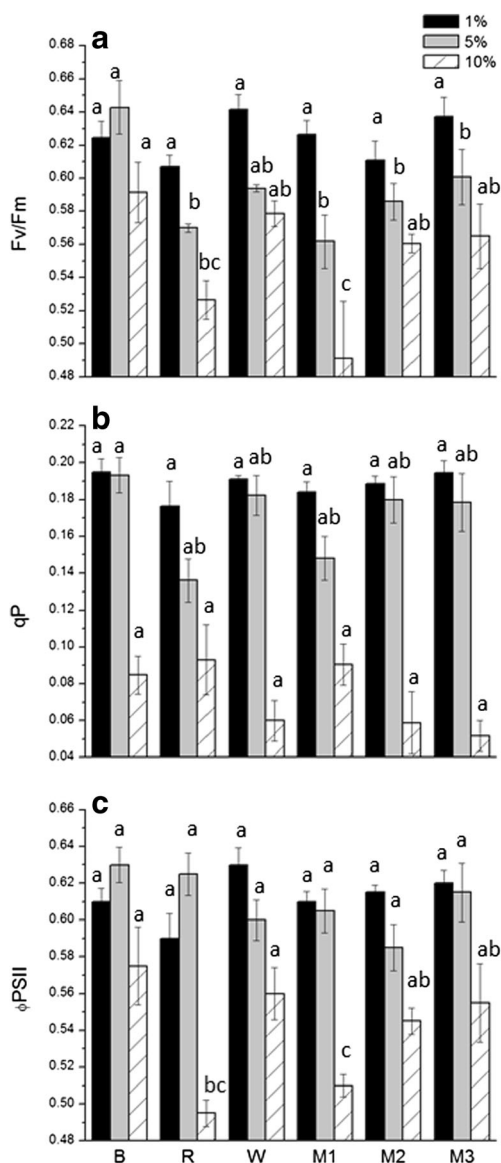


Fig. 4 *Micractinium inermum* **a** maximum quantum yield of photosystem II (F_v/F_m), **b** photochemical quenching (qp), and **c** ϕ PSII, the photochemical yield of electron transport of open PSII reaction centers, under different spectral light treatments and CO₂ concentrations during the exponential phase. Data represent means ($n = 4 \pm$ SD). Values within the same bar pattern with different letters represent a significant difference ($p < 0.05$)

cannot reliably report q_N or NPQ values (Campbell et al. 1998). We were, however, able to use the highest F_m' level acquired to determine that relative NPQs were in the range of 0.2 to 0.4 and did not show any significant findings among light treatments ($p = 0.534$).

Statistical analyses of chlorophyll *a* and *b* and carotenoids showed significant interactions between light quality and carbon dioxide during the exponential ($p < 0.001$, $p = 0.005$, $p < 0.001$, respectively) and stationary phases ($p < 0.001$, $p < 0.001$, $p < 0.001$, $p < 0.001$) determined by two-way ANOVA. The increase in photon capture efficiency in blue light was

accompanied by increased amounts of pigments compared with the amounts in red light. During the exponential phase in 1 and 5% CO₂, chlorophyll *a* (Chl*a*) was at least 1.2× greater in blue light than red light ($p < 0.001$, $p = 0.013$) (Fig. 5). At the stationary phase, that difference in Chl*a* between blue and red light increased to ~2× or more ($p < 0.001$, $p < 0.001$). Cultures grown in blue light contained significantly greater Chl*b* and total carotenoid content than those grown in red light during the exponential phase at 5% ($p < 0.001$) and during the stationary phase at 1, 5, and 10% CO₂ ($p < 0.001$). There was a noticeable trend of increasing cellular Chl*a*, Chl*b*, and carotenoid content with the treatments as the red/blue ratios decreased, consistent with an increasing blue wavelength peak. When examining the stationary phase samples, as CO₂ increased, total pigment content decreased and was significantly different between 5 and 10% ($p < 0.001$) (Fig. 5).

Statistical analyses of protein results showed a significant interaction between CO₂ and light treatments ($p < 0.001$). Variation in cellular composition was found due to the stress of increased carbon dioxide levels ($p < 0.001$) and by the spectral distribution of light generally although there was a significant difference in protein content at 10% CO₂ between blue and red light treatments that may indicate that blue light is relevant under conditions of stress (Table 4). Protein content decreased with increasing CO₂ concentrations, and simultaneously total carbohydrate concentration increased (Table S2 in Supplemental Data). Protein content was significantly higher in the exponential phase than in the stationary phase although the resulting difference lessened as CO₂ levels increased because cells were already growth inhibited due to stress. Although significant differences were observed in total FAME content ($p < 0.001$) among LED and CO₂ treatments, the repeatability of this analysis is very high and the actual percent differences are quite small. In addition, there does not seem to be a pattern to the differences that would suggest a large effect (Table S1 in Supplemental Data). In addition, no significant differences were uncovered with a more detailed examination of the individual fatty acids. Data were pooled into saturated fatty acids (SFA), monosaturated fatty acids (MUFA), and polyunsaturated fatty acids (PUFA) and depicted in Fig. 6. There is an interaction between LED and CO₂ treatments on carbohydrate content during both exponential and stationary phases ($p < 0.001$, $p < 0.001$), and there is a trend towards a greater carbohydrate content in red light versus blue light; however, the differences are not significant (Table S2 in Supplemental Data). A point of note though, carbohydrate content was calculated by subtracting the other main chemical components as mentioned in “Materials and methods”. Pigments were not included in that calculation because there was insufficient biomass to analyze pigments from the exponential

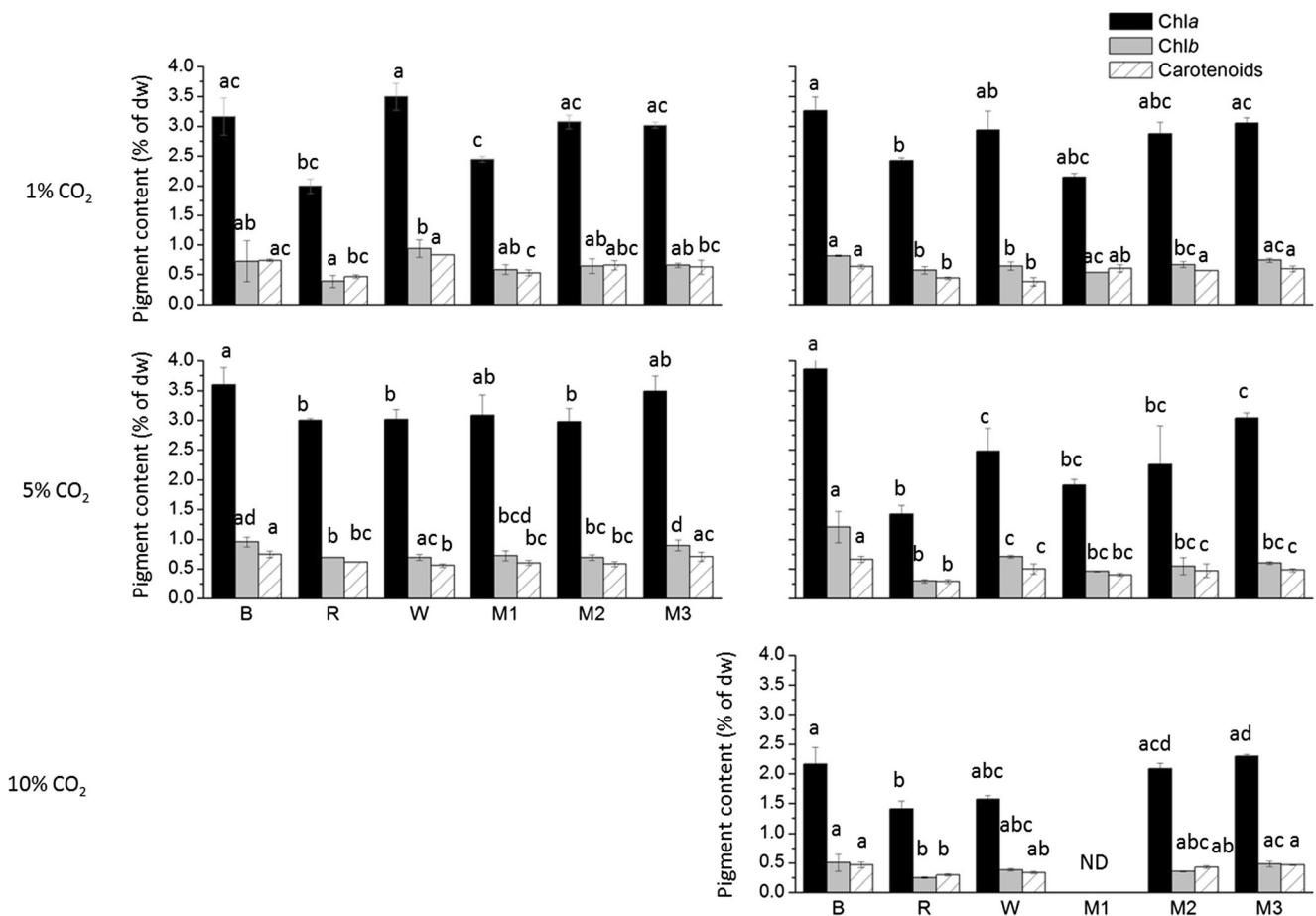


Fig. 5 Chlorophyll *a* and *b* and total carotenoids of *Micractinium inermum* under 3 different CO₂ concentrations (1%, 5%, and 10%) and 6 light treatments during the exponential (E, column on the left) and stationary phases (S, column on the right). There was insufficient

biomass available to sample during the exponential phase at 10% CO₂. M1 treatment cultures at 10% CO₂ crashed. Data represent means ($n = 6 \pm \text{SD}$). Values within the same bar pattern with different letters represent a significant difference ($p < 0.05$)

sampling point of 10% CO₂. The significant differences in pigment quantity found among LED treatments (Fig. 5) could therefore impact the carbohydrate values.

Discussion

The results presented here show that spectral light quality provided by LEDs caused considerable differences in the growth kinetics of *Micractinium inermum*, and a compounding effect was shown when grown with different CO₂ concentration treatments. Cultures irradiated with blue light were less negatively affected as the CO₂ concentration increased compared with red light grown cultures. This effect correlated with the relative amount of blue light used to grow the cells. Previous research has revealed that microalgal cells have demonstrated optimal growth and high biofixation rates when aerated with high concentrations of CO₂. Tang et al. (2011) for example, found that in *Scenedesmus obliquus* and in *Chlorella*

pyrenoidosa, the best growth potential was observed at 10% CO₂. Yoo et al. (2010) similarly demonstrated that *Chlorella vulgaris* and *Scenedesmus* sp. could be cultivated with up to 10% CO₂ without adverse effects on growth. On the other hand, a significant lag phase was shown by *Botryococcus braunii* at 10% as the culture adapted to the higher level of CO₂. In the present study, as CO₂ increased from 1 to 5 to 10%, *M. inermum* cultures demonstrated decreased photosynthetic efficiency, growth rates, and productivity. As with Tang et al. (2011) and Yoo et al. (2010), the cultures here were not acclimated to the CO₂ treatment concentration prior to experimentation. Our aim was to capture the tolerance of the microalgae without pre-acclimation to mimic conditions found at the industrial scale where flue gas application can be unpredictable, often decreasing to ambient air CO₂ levels for periods of time. Similar to our findings, many research studies have shown that CO₂ levels above 2% could damage microalgal cells and inhibit growth (Chiu et al. 2009). This inhibition of growth can in part be attributed to the inhibition of

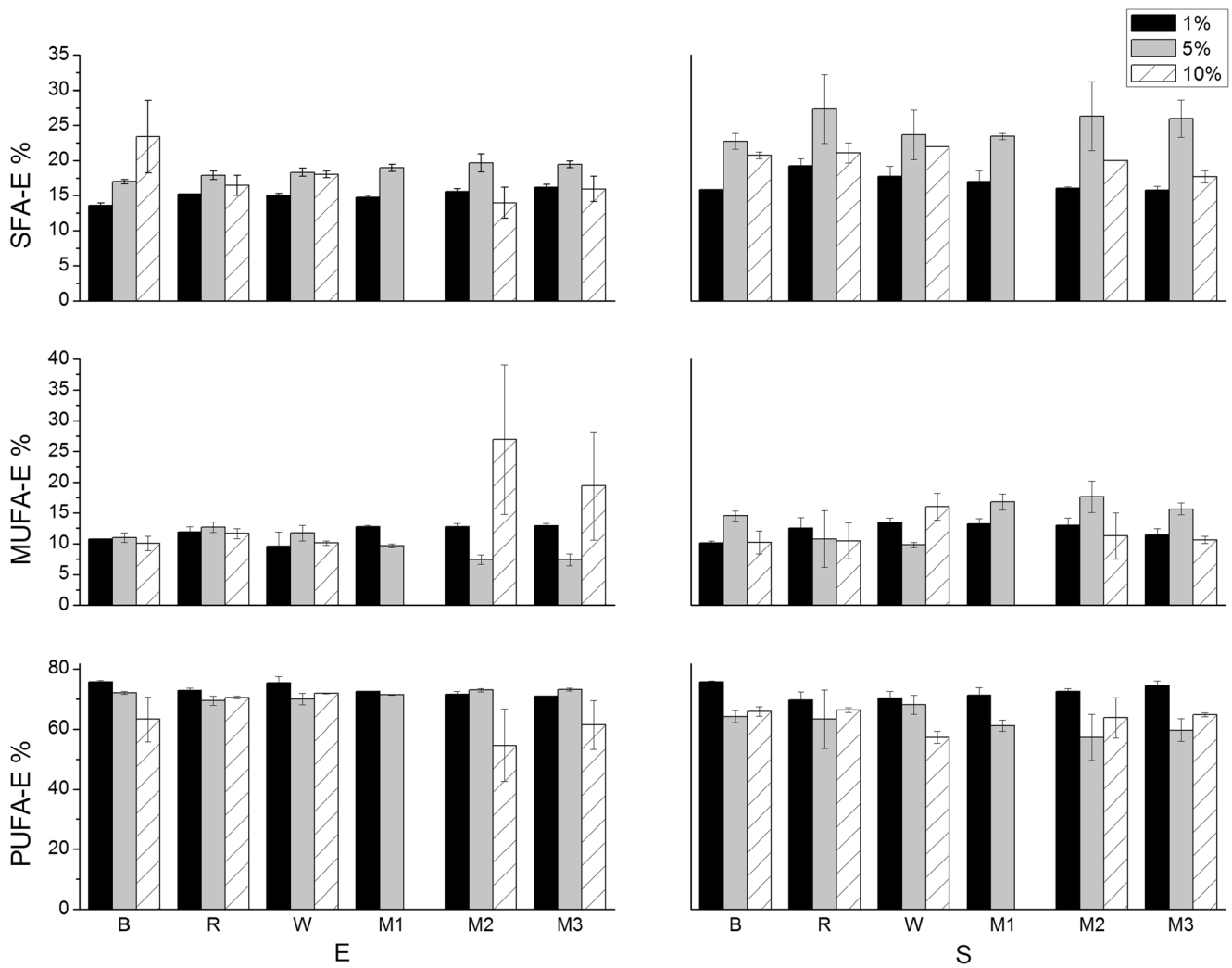


Fig. 6 Saturated fatty acid (SFA), monosaturated fatty acid (MUFA), and polyunsaturated fatty acid (PUFA) content (% of total fatty acids) under 3 different CO₂ concentrations (1%, 5%, and 10%) and 6 light treatments

during the exponential (E, column on the left) and stationary phases (S, column on the right)

photosystem II function found at high CO₂ levels in our study beyond 1%, to 5 then 10. The photochemical quenching parameter q_p reveals how open or closed PSII centers are based on excitation of the centers and the removal of electrons via the electron transport chain (Campbell et al. 1998). The low q_p values found here generally can therefore be explained by the low light levels available for excitation of the PSII centers. In addition, energy consumption can be affected by factors slowing electron removal (Campbell et al. 1998), and this was evident in the further reduction of q_p and the suppression of ϕ_{PSII} with CO₂ stress. This inhibition of photosynthesis correlated with a decreased carbon dioxide fixation rate.

Our study clearly shows that the stress of increased CO₂ had a greater impact on cellular growth characteristics in the red light treatment than when a blue light peak with a range of 410–500 nm was applied. Interestingly, the

percentage of blue light during growth often impacted both growth kinetics and photosynthetic parameters. A reduction in PSII activities revealed by the reduction in maximum efficiency of PSII photochemistry (F_v/F_m) was observed in the red light treatment and increased as the ratio of red to blue light decreased. This increasing response to blue light was characterized by Hogewoning et al. (2010) as a blue light quantitative effect rather than just a qualitative result. The observed differences in F_v/F_m among light treatments may be attributed to the corresponding variation in pigment content that will be discussed further. The inclusion of a blue wavelength peak (450 nm) in the spectra demonstrated a greater μ_{max} than red at 5 and 10% CO₂ where culture stress was evident, and the same blue light quantitative pattern emerged. A lower μ_{max} in cultures grown in red light alone has been shown for different algal species. Das et al. (2011) found that with

Nannochloropsis sp., the maximum specific growth rate was highest in order of blue, white, green, and then red. *Tisochrysis lutea* was found to have the highest growth rates while grown in blue and white light and lowest rates with green and red light (Sanchez-Saavedra et al. 2016). Katsuda et al. (2004), similar to our study, demonstrated that blue light enhanced growth in the early exponential phase but then showed growth suppression later on compared with red LEDs. Interestingly, there were longer lag phases in R, M1, and M2 that increased dramatically with added stress. At a 10% CO₂ concentration, RGR of R, M1, and M2 decreased significantly and in some cases (R and M1) cell cultures were no longer able to overcome growth inhibition and cultures crashed. We have therefore demonstrated a pattern that suggests that a blue wavelength peak in the spectra is advantageous in the early exponential stage of growth and may additionally augment tolerance to changes in the environment early on and that this effect is quantitative in terms of the peak area percentage. Conversely, a red wavelength peak in the spectra is shown to allow for *M. inermum* cultures to ultimately achieve a higher biomass concentration by the stationary phase; these cultures are able to catch up (as observed with RGR) and then surpass, also following a quantitative pattern of red peak area percentage. Interestingly, our W treatment includes a green wavelength peak in addition to blue and red that also plays a role, further enhancing growth kinetics in early exponential phase. Mattos et al. (2015) reported the importance of green light with cultures of *Scenedesmus bijuga*. They demonstrated that as culture density and light path increased, red and blue light was absorbed more readily by chlorophyll pigments and green light was able to irradiate more cells deeper into the culture. They theorize that the weakly absorbed green wavelengths maximize overall production efficiency (Mattos et al. 2015) which was also evident in our study.

The growth advantage observed in cultures subjected to a blue wavelength peak in the early exponential phase is clear and is enhanced, or imperative for culture survival in some cases with increasing environmental CO₂ stress. This gain may in part be contributed by the increased amounts of pigments that were formed in response to blue LEDs (Wallen and Geen 1971). Light spectral composition plays an important role in photosynthesis and therefore influences development and metabolism (Wu 2016). There is a paucity of information in this area; however, it has been demonstrated that an increased production of pigments, RNA, and DNA were associated with increased plastids, thylakoid stacks per chloroplast, and photosynthetic capacity of the cells in blue light (Round 1984). The decrease in the Chl*a*/Chl*b* ratio seen in blue light compared with red light grown cells can be explained by the greater absorption of chlorophyll *b* in the 400–500-nm range than chlorophyll *a* (Hess and Tolbert

1967). It is also possible that the beneficial effect observed is due to the cell's ability to repair damage (Ruyters 1984). The enhanced production of pigments discussed includes photoprotective pigments that are formed to protect the photosynthetic apparatus (Shultze et al. 2014). The production of reactive oxygen species (ROS) has been shown to be caused by stressful environmental factors such as high levels of CO₂ (Mallick and Mohn 2000) and may be a cause contributing to the long lag phases and suppressed growth observed here. It has been demonstrated that cellular metabolic pathways are influenced by spectral quality and specifically by blue light (Rivkin 1989; Ruyters 1984; Rossa et al. 2002). Rossa et al. (2002), for example, has demonstrated that activities of superoxide dismutase, an important antioxidant enzyme, are higher in blue light than red. A detoxification mechanism such as this may explain our observations. Furthermore, blue light can be absorbed more efficiently than red light, and in this case, the blue LED emitted matches up nicely to the blue wavelength peak range of the absorption spectrum for *M. inermum* (410–500 nm). For green algae, the major wavelengths for light utilization are within the ranges of 420–470 nm and 660–680 nm with accessory pigments outside of these ranges (Carvalho et al. 2011). As biomass concentration increased, light treatments with red peaks were more optimal than blue for biomass production. Although there is overlap, the red light wavelength range of 590–660 nm (maximum peak at 630 nm) used in this study (Fig. 1) does not match up as nicely to the red peak range of the absorption spectrum of 630–684 nm (maximum peak at 660 nm) (Fig. 2). Since red light is absorbed strongly by chlorophyll *a* at 662 nm, it is possible that photons outside of the range are able to penetrate deeper into the culture increasing the efficiency of their use translating into increased biomass concentration. The same rationale was described by Mattos et al. (2015) in terms of green light. Red light of 630 and 660 nm has however been shown to result in high biomass productivity compared with blue or white light for *Tetraselmis* sp. and *Chlorella* sp. (Yan et al. 2013; Zhao et al. 2013; Abiusi et al. 2014). Further studies comparing LEDs at both 630 nm and 660 nm would be useful to determine whether or not tailoring the red light emission to the absorption spectra of the microalga is important in order to maximize photosynthetic efficiency in the lag and exponential phases.

Sampling for biochemical composition occurred at a specific point for both exponential and stationary sample points relative to the growth curve and not time. This allowed us to compare protein, carbohydrate, and fatty acid content based solely on spectral distribution and carbon dioxide concentration without the confounding variables of growth kinetics. This meant that although it may have taken treatments with red peaks longer (longer lag phase) to get to the exponential phase than treatments with blue peaks, once in the exponential phase the biochemical composition did not differ greatly

among them. Protein content was higher in blue light at 10% CO₂ than in white or red light corresponding to a decrease in carbohydrates. The observation of increased protein in blue light was found by Shulze and was explained by two possible factors: (1) blue light is known to cause the degradation of carbohydrates and (2) the accumulation of pigments found in blue light under conditions of stress will increase their light harvesting complex proteins. The decrease in protein and the corresponding increase in storage components found with increased CO₂ levels are typical under conditions of stress as growth slows and was further evidenced by the slowing of growth in the stationary phase versus the exponential phase.

Cultivation systems designed to recycle CO₂ from flue gas aim for the capture of large quantities of CO₂ to achieve economic viability. Based on this investigation, a greater CO₂ fixation rate occurred at the lowest CO₂ concentration applied regardless of the light spectrum. There is therefore no benefit in subjecting a *M. inermum* culture to an inflow of flue gas with a higher CO₂ level. Any additional CO₂ would be released into the head space of the PBR and would negatively affect the efficiency of growth and the effectiveness of carbon recycling.

Conclusions

Effects were observed on photosynthetic efficiencies and growth kinetics of *M. inermum* by changes in the spectral light quality and the CO₂ concentration applied. Due to the advantages of reduced lag phase and a greater tolerance to CO₂ stress in early growth, a strategy of incorporating blue light into the design of microalgal cultivation systems may impact overall productivity. Findings from this investigation suggest that an optimized method of applying two stages of irradiance, where applying monochromatic blue light at the onset of cultivation is the first stage and then switching during the exponential phase to monochromatic red LEDs is the second stage, with more weakly absorbed green wavelengths included in both stages, would allow for greater CO₂ fixation and biomass productivity without having much effect on the biochemical composition of the product. Differences in the biochemical composition among light treatments were not enough to warrant choosing specific LEDs for the purpose of enhancing a specific component. A decreased tolerance to CO₂ levels above 1% suggests that under the same environmental conditions, flue gas should be diluted for optimal results.

Acknowledgments The authors wish to thank Laura Garrison and Cheryl Wall for their technical support during this study. We gratefully acknowledge Sean Tibbetts and Shane Patelakis for reviewing a draft of this manuscript.

Funding information Funding for this work was provided by NRC's Algal Carbon Conversion Program. This is NRC publication no. 56441.

References

- Abiusi F, Sampietro G, Marturano G, Biondi N, Rodolfi L, D'Ottavio M, Tredici MR (2014) Growth, photosynthetic efficiency, and biochemical composition of *Tetraselmis suecica* F&M-M33 grown with LEDs of different colors. *Biotechnol Bioeng* 111:956–964
- Baer S, Heining M, Schwerna P, Buchholz R, Hübner H (2016) Optimization of spectral light quality for growth and product formation in different microalgae using a continuous photobioreactor. *Algal Res* 14:109–115
- Beardall J, Johnston A, Raven J (1998) Environmental regulation of CO₂-concentrating mechanisms in microalgae. *Can J Bot* 76:1010–1017
- Borodin V, Gardeström P, Samuelsson G (1994) The effect of light quality on the induction of efficient photosynthesis under low CO₂ conditions in *Chlamydomonas reinhardtii* and *Chlorella pyrenoidosa*. *Physiol Plant* 92:254–260
- Campbell D, Hurry V, Clarke AK, Gustafsson P, Öquist G (1998) Chlorophyll fluorescence analysis of cyanobacterial photosynthesis and acclimation. *Microbiol Mol Biol Rev* 62:667–668 3
- Carvalho AP, Silva SO, Baptista JM, Malcata FX (2011) Light requirements in microalgal photobioreactors: an overview of biophotonic aspects. *Appl Microbiol Biotechnol* 89:1275–1288
- Chaloub RM, Reinert F, Nassar CG, Fleury BG, Mantuano DG, Larkum AWD (2010) Photosynthetic properties of three Brazilian seaweeds. *Rev Bras Bot* 33:371–374
- Chiu SY, Kao CY, Tsai MT, Ong SC, Chen CH, Lin CS (2009) Lipid accumulation and CO₂ utilization of *Nannochloropsis oculata* in response to CO₂ aeration. *Bioresour Technol* 100:833–838
- Cuellar-Bermudez SP, Garcia-Perez JS, Rittman BE (2015) Photosynthetic bioenergy utilizing CO₂: an approach on flue gases utilization for third generation biofuels. *J Clean Prod* 98:53–65
- Das P, Lei W, Aziz SS, Obbard JP (2011) Enhanced algae growth in both phototrophic and mixotrophic culture under blue light. *Bioresour Technol* 102:3883–3887
- Dickinson KE, Whitney CG, McGinn PJ (2013) Nutrient remediation rates in municipal wastewater and their effect on biochemical composition of the microalga *Scenedesmus* sp. AMDD. *Algal Res* 2: 127–134
- Guillard RRL, Ryther JH (1962) Studies of marine planktonic diatoms. I. *Cyclotella nana* Hustedt and *Detonula confervacea* (Cleve) Gran. *Can J Microbiol* 8:229–239
- Hess JL, Tolbert NE (1967) Changes in chlorophyll a/b ratio and products of ¹⁴CO₂ fixation by algae grown in blue or red light. *Plant Physiol* 42:1123–1130
- Hogewoning SW, Trouwborst G, Maljaars H, Poorter H, van Ieperen W, Harbinson J (2010) Blue light dose-responses of leaf photosynthesis, morphology, and chemical composition of *Cucumis sativus* grown under different combinations of red and blue light. *J Exp Bot* 61:3107–3117
- Janssen M, Tramper J, Mur LR, Wijffels RH (2002) Enclosed outdoor photobioreactors: light regime, photosynthetic efficiency, scale-up, and future prospects. *Biotechnol Bioeng* 81:193–210
- Jeffrey SW, Humphrey GF (1975) New spectrophotometric equations for determining chlorophylls a, b and c₁ and c₂ in higher plants, algae and natural phytoplankton. *Biochem Physiol Pflanz* 167:191–194
- Katsuda T, Lababpour A, Shimahara K, Katoh S (2004) Astaxanthin production by *Haematococcus pluvialis* under illumination with LEDs. *Enzym Microb Technol* 35:81–86
- Kumar K, Banerjee D, Das D (2014a) Carbon dioxide sequestration from industrial flue gas by *Chlorella sorokiniana*. *Bioresour Technol* 152: 225–233
- Kumar MS, Hwang J, Abou-Shanab RAI, Kabra AN, Ji M, Jeon B (2014b) Influence of CO₂ and light spectra on the enhancement of microalgal growth and lipid content. *J Renew Sustain Energy* 6: 063107

- Laurens LML, Dempster TA, Jones HDT, Wolfrum EJ, Van Wychen S, McAllister JSP, Rencenberger M, Parchert KJ, Gloe LM (2012) Algal biomass constituent analysis: method uncertainties and investigation of the underlying measuring chemistries. *Anal Chem* 84:1879–1887
- Lourenço SO, Barbarino E, Laviñ PL, Marquez UML, Aidar E (2004) Distribution of intracellular nitrogen in marine microalgae: calculation of new nitrogen-to-protein conversion factors. *Eur J Phycol* 39:17–32
- Mallick N, Mohn FH (2000) Reactive oxygen species: response of algal cells. *J Plant Physiol* 157:183–193
- Mattos ER, Singh M, Cabrera ML, Das KC (2015) Enhancement of biomass production in *Scenedesmus bijuga* high-density culture using weakly absorbed green light. *Biomass Bioenergy* 81:473–478
- Packer M (2009) Algal capture of carbon dioxide; biomass generation as a tool for greenhouse gas mitigation with reference to New Zealand energy strategy and policy. *Energy Policy* 3428:3437
- Pienkos PT, Darzins A (2009) The promise and challenges of microalgal-derived biofuels. *Biofuels Bioprod Bioursour* 3:431–440
- Pires JCM, Alvim-Ferraz MCM, Martins FG, Simões M (2012) Carbon dioxide capture from flue gases using microalgae: engineering aspects and biorefinery concept. *Renew Sustain Energy Rev* 16:3043–3053
- Rossa MM, de Oliveira MC, Okamoto OK, Lopes PF, Colepicolo P (2002) Effect of visible light on superoxide dismutase (SOD) activity in the red alga *Gracilariopsis tenuifrons* (Gracilariales, Rhodophyta). *J Appl Phycol* 14:151–157
- Rivkin RB (1989) Influence of irradiance and spectral quality on the carbon metabolism of phytoplankton I. Photosynthesis, chemical composition and growth. *Mar Ecol Prog Ser* 55:291–304
- Round FE (1984) *The ecology of algae*. Cambridge University Press, Cambridge, pp 353–355
- Ruiz J, Oliveira G, de Vree J, Bosma R, Willems P, Reith JH, Eppink MHM, Kleinegris DMM, Wijffels RH, Barbosa MJ (2016) Towards industrial products from microalgae. *Energy Environ Sci* 9:3036–3043
- Ruyters G (1984) Effects of blue light on enzymes. In: Senger H (ed) *Blue light effects in biological systems*. Springer, Berlin, pp 283–301
- Sanchez-Saavedra MD, Maeda-Martinez AN, Acosta-Galindo S (2016) Effect of different light spectra on the growth and biochemical composition of *Tisochrysis lutea*. *J Appl Phycol* 28:839–847
- Shultze PSC, Barreira LA, Pereira HGC, Perales JA, Varela JCS (2014) Light emitting diodes (LEDs) applied to microalgal production. *Trends Biotechnol* 32:422–430
- Strickland JDH, Parsons TR (1968) *A practical handbook of seawater analysis*. Bull Fish Res Bd Can 167:1–310
- Tang D, Han W, Li P, Miao X, Zhong J (2011) CO₂ biofixation and fatty acid composition of *Scenedesmus obliquus* and *Chlorella pyrenoidosa* in response to different CO₂ levels. *Bioresour Technol* 102:3071–3076
- Tibbetts SM, Milley JE, Lall SP (2015a) Chemical composition and nutritional properties of freshwater and marine microalgal biomass cultured in photobioreactors. *J Appl Phycol* 27:1109–1119
- Tibbetts SM, Whitney CG, MacPherson MJ, Bhatti S, Banskota AH, Stefanova R, McGinn PJ (2015b) Biochemical characterization of microalgal biomass from freshwater species isolated in Alberta, Canada for animal feed applications. *Algal Res* 11:435–447
- Umino Y, Satoh A, Shiraiwa Y (1991) Factors controlling induction of external carbonic anhydrase and change in K_{1/2}(CO₂) of photosynthesis in *Chlorella regularis*. *Plant Cell Physiol* 32:379–384
- Wallen DG, Geen GH (1971) Light quality in relation to growth, photosynthetic rates and carbon metabolism in two species of marine plankton algae. *Mar Biol* 10:34–43
- Wijffels RH, Barbosa MJ (2010) An outlook on microalgal biofuels. *Science* 329:796–799
- Wu H (2016) Effect of different light qualities on growth, pigment content, chlorophyll fluorescence, and antioxidant enzyme activity in the red alga *Pyropia haitanensis* (Bangiales, Rhodophyta). *Biomed Res Int* 2016:8
- Yan C, Zhang L, Luo X, Zheng Z (2013) Effects of various LED light wavelengths and intensities on the performance of purifying synthetic domestic sewage by microalgae at different influent C/N ratios. *Ecol Eng* 51:24–32
- Yoo C, Jun S, Lee J, Ahn C, Oh H (2010) Selection of microalgae for lipid production under high levels of carbon dioxide. *Bioresour Technol* 101:71–74
- Yun Y, Lee SB, Park JM, Lee C, Yang J (1997) Carbon dioxide fixation by algal cultivation using wastewater nutrients. *J Chem Technol Biotechnol* 69:451–455
- Zhao Y, Wang J, Zhang H, Yan C, Zhang Y (2013) Effects of various LED light wavelengths and intensities on microalgae-based simultaneous biogas upgrading and digestate nutrient reduction process. *Bioresour Technol* 136:461–468

Publisher's note Springer Nature remains neutral with regard to jurisdictional claims in published maps and institutional affiliations.